Engineering Structures 162 (2018) 166–176

Contents lists available at ScienceDirect

Engineering Structures

journal homepage: www.elsevier.com/locate/engstruct

Artificial neural network based multi-dimensional fragility development of skewed concrete bridge classes

Sujith Mangalathu[a], Gwanghee Heo[b], Jong-Su Jeon[c,*]

[a] Department of Civil and Environmental Engineering, University of California, Los Angeles, CA 90095, USA
[b] Department of International Civil and Plant Engineering, Konyang University, Nonsan, Chungcheongnam-do 32992, Republic of Korea
[c] Department of Civil Engineering, Andong National University, Andong, Gyeongsangbuk-do 36729, Republic of Korea

ARTICLE INFO

Keywords:
Bridge skew
Concrete box-girder bridges with seat abutments
Artificial neural network
Multi-dimensional fragility curves
Regional risk assessment

ABSTRACT

Recent researches are directed towards the regional seismic risk assessment of structures based on a bridge inventory analysis. The framework for traditional regional risk assessments consists of grouping the bridge classes and generating fragility relationships for each bridge class. However, identifying the bridge attributes that dictate the statistically different performances of bridges is often challenging. These attributes also vary depending on the demand parameter under consideration. This paper suggests a multi-parameter fragility methodology using artificial neural network to generate bridge-specific fragility curves without grouping the bridge classes. The proposed methodology helps identify the relative importance of each uncertain parameter on the fragility curves. Results from the case study of skewed box-girder bridges reveal that the ground motion intensity measure, span length, and column longitudinal reinforcement ratio have a significant influence on the seismic fragility of this bridge class.

1. Introduction

One common approach to assess the seismic vulnerability is through the derivation of fragility curves. Fragility curves gives the likelihood that a structure or its components will reach a certain level of damage for a given ground motion intensity measure (IM). The usual strategy adopted to generate bridge class fragilities is to bin the bridges that have statistically similar performances and sample bridge classes in each group accounting for the variation in structural, material, and geometric attributes, and generate the fragility curves.

Numerous studies have been carried out to group bridge classes and suggest their fragility relationships [1–9]. HAZUS [1] is the most comprehensive document in grouping the bridge classes and suggested fragility relationships. However, the fragility relationships suggested in HAZUS are based on simple two-dimensional (2-D) analyses of bridges and do not reflect the material, structural, and geometric uncertainties. Mangalathu et al. [2] outlined the limitations of HAZUS fragilities such as the grouping of bridge classes based on engineering judgement and the use of capacity spectrum method to generate the fragility curves. Mackie and Stojadinovic [3] partially addressed the limitation of HAZUS and suggested fragility relationships for some specific bridge classes accounting for the variation in geometric properties. Banerjee and Shinozuka [4,5] suggested fragility relationships for bridge classes by grouping the bridge classes based on the number of spans (single versus multiple), bent type (single versus multiple), and skew angle (negligible versus significant, chosen to be > 30°). Ramanathan [6] classified the bridge classes in California based on the superstructure type, number of columns, design era, and abutment configurations, and suggested their fragility relationships. As noted by Mangalathu et al. [7], the above mentioned studies classified the bridge classes based on the engineering judgment which is subjective. These authors suggested a performance-based grouping based on a statistical technique called analysis of covariance. However, the scope of their study was limited to grouping bridge classes, not the generation of fragility curves. Mangalathu [8] suggested fragility relationships of California concrete bridges after grouping the bridge classes based on the structural response via the analysis of variance. This author classified the bridge classes based on the abutment type, pier-type, number of spans, column cross-section, span continuity, and seismic design. In all the aforementioned studies, the fragility relationships were conditioned only on IM. However, recent researches [10–13] highlighted that the fragility relationships conditioned on a single parameter (IM) might not be enough to capture uncertainties associated with other input parameters. The single-parameter fragility curves also suffer the limitation that it requires extensive re-simulation to update the fragility curves for a new set of input parameters.

* Corresponding author.
E-mail addresses: sujithmangalath@g.ucla.edu (S. Mangalathu), heo@konyang.ac.kr (G. Heo), jsjeon@anu.ac.kr (J.-S. Jeon).

https://doi.org/10.1016/j.engstruct.2018.01.053
Received 10 August 2017; Received in revised form 8 October 2017; Accepted 18 January 2018
Available online 17 February 2018

To mitigate the limitations of traditional single-dimensional fragility curves, recent researches [10–17] suggested multi-dimensional fragility curves, i.e., the fragility relationships are conditioned on input parameters including uncertain geometric, material, and structural parameters, in addition to IM. The multi-parameter fragility curves are generated using logistic regression on the demand-to-capacity estimates. However, the multi-parameter fragility curves are generated after an initial classification of bridges based on either engineering judgment or statistical performance. The performance based grouping of bridge classes is not always possible if one would like to perform the regional risk assessment of bridges with less computational efforts. As noted by Mangalathu [8], bridge attributes that dictate the bridge performance vary depending on the component under consideration, and the generation of fragility relations for the refined bridge group accounting for all the attributes is computationally expensive.

A few researchers [18–22] applied artificial neural network (ANN) in the field of structural engineering to estimate structural damage and seismic fragilities. ANN is one of machine learning techniques on the basis of a large connection of simple units called neurons, similar to axons in human brain [23]. It consists of an input layer of neurons (or nodes, units), hidden layers of neurons, and a final layer of output neurons. ANN has the capability in capturing the nonlinear behavior, and has an efficient input-out mapping. [23]. Compared to other machine learning methods such as Random Forest, ANN is robust in the presence of noisy or missing inputs and have the adaptively to learn in changing environment [23]. The comparison of the efficiency of ANN with other machine learning techniques is beyond the scope of the current study. Lagaros and Fragiadakis [18] evaluated the application of neural network–based methodology for a rapid estimation of the seismic demand of steel frames. Lautour and Omenzetter [19] explored the application of ANN in evaluating damage indices of 2-D reinforced concrete frames. Mitropoulou and Papadrakakis [20] generated fragility curves for buildings using ANN. The research by these authors pointed out that the computation time in the traditional fragility analysis can be reduced significantly with the use of ANN. Lu and Zhang [21] compared the fragility curve of steel buildings obtained by ANN and finite element analysis (FEA). These authors noted that if a sufficient amount of training data is available (with a set of 500 data points), ANN can produce accurate estimates of fragilities with less computational time compared to FEA. Pang et al. [22] simulated the median value and standard deviation of incremental dynamic analysis curves at various levels of IM using ANN.

This research employs ANN to generate fragility curves for bridge classes in California. Unlike previous studies on the application of machine learning techniques for bridge fragilities [8,10], this research explores the use of ANN without grouping bridge classes based on skew angle, number of spans and columns per bent. Unlike previous studies on the application of machine learning techniques for bridge fragilities [8,10], this research explores the use of ANN without grouping bridge classes based on skew angle, number of spans and columns per bent. Per Mangalathu [8], eight bridges classes with statistically different performances are possible with these combinations (the number of columns per bent: one versus two, abutment skewness: straight versus skewed, the number of spans: two-span versus three-to-four-span). Especially, skewed bridges can be classified into five different bins based on their response: low (0–15°), medium (15–30°), high (30–45°), very high (45–60°), and extreme (60–77°) [24]. The establishment of a predictive equation between uncertain input (modeling) parameters and output (structural response) parameter enable to perform the rapid risk assessment and generation of bridge-specific fragility curves for a set of input parameters. To examine the capability of ANN, this research selects two-span, three-span, and four-span skewed box-girder bridges with single-column and two-column bents and with seat abutments. Thus, 20 (five levels of skew angle × two types of column bent × two numbers of span) bridge classes are possible with these combinations. The skewed bridges occupy more than 60% of the California bridge inventory, and their risk assessment is getting considerable attention these days [24–28]. The scope of the study is limited to seismically designed (constructed after 1970) pre-stressed concrete box-girder bridges with seat abutments.

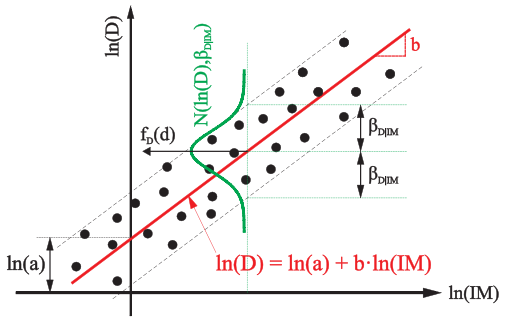

Fig. 1. Illustration of single-parameter PSDM.

2. Proposed probabilistic seismic demand models

2.1. Traditional probabilistic seismic demand models

The probabilistic seismic demand model (PSDM) is a linear regression of pairs of input (demand, *D*) and output (*IM*) variables in the log-transformed space. Fig. 1 shows the scatter plot of the seismic demand or response (*D*) of a bridge group versus the *IM* in the logarithmic space, along with the probability distribution of the seismic demands. Note that the PSDM shown in the figure is single parameterized, i.e., conditioned only on IM. Per Cornell et al. [29], the PSDM can be written as

$$\ln(S_d) = \ln(a) + b\ln(IM) \tag{1}$$

where a and b are the regression coefficients, S_d is the median estimate of the demand in terms of *IM*. The coefficients a and b are obtained by performing a linear regression analysis on *D* and *IM* pairs in the logarithmic space. Dispersion, $\beta_{d|IM}$, is evaluated based on statistical analysis of ln(*D*) and ln(*IM*) pairs:

$$\beta_{d|IM} = \sqrt{\frac{1}{N-2}\sum_{i=1}^{N}[\ln(d_i)-\ln(S_d)]^2} \tag{2}$$

where d_i is the demand for the ith ground motion and N is the number of dynamic analyses.

2.2. Artificial neural network for probabilistic seismic demand models

ANN is a mathematical model inspired by the organization and functioning of biological neurons. The data from the dynamic analyses are split randomly in this research into a training set (70%), a validation set (15%), and a test set (15%). ANN consists of the input layer, hidden layer, and output layer, as shown in Fig. 2. Each line connecting neurons is associated with a weight. The output (h_i) of the neuron i in the hidden layer is

$$h_i = s\left(\sum_{j=1}^{N} V_{ij}x_j + T_i^{hid}\right) \tag{3}$$

where $s()$ is called the activation or transfer function. N is the number of input neurons, V_{ij} is the weights, x_j is the input value, and T_i^{hid} is the threshold term of hidden neurons. The activation function used in this research is sigmoid to introduce the nonlinearity in the model [23,30] and is defined as

$$s(u) = \frac{1}{1+e^{-u}} \tag{4}$$

The network is trained with the training data to minimize the error function in predicting the demand model, by adjusting the weights

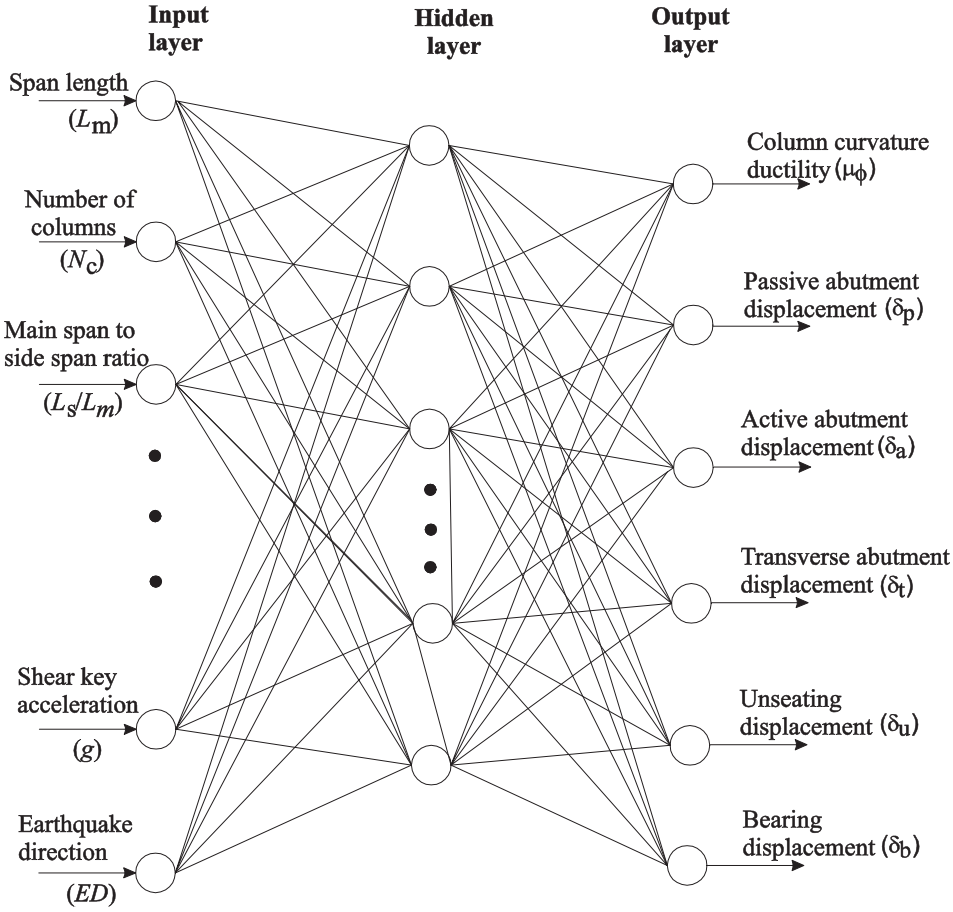

Fig. 2. Layout for artificial neural network for the prediction of demand model.

between the connected neurons. The validation test is then performed to find the optimal weights, and the efficiency of the network is estimated using the test set. The input parameters used here consist of categorical variables (e.g., the number of columns per bent, backfill type), numerical variables (e.g., the number of spans, the number of columns), and continuous variables (e.g., span length, concrete compressive strength). The output of ANN is the seismic demand of bridge components. The efficiency of ANN depends on the number of hidden layers and neurons. Following the recommendation of Wang [30], one hidden layer with 10 neurons is used in this research. A sensitivity study showed that adding more hidden layers and increasing neurons in the hidden layer beyond 10 does not affect the results, and thus 10 neurons are used in this research. Interested readers are directed to Haykin [23] for a more detailed discussion on the requirements of the number of hidden layers and neurons.

To evaluate the efficiency of ANN compared to the traditional single-parameter fragility analysis, two case studies have been performed. The first case study, two-span bridges with seat abutments are considered to examine the comparison of ANN-based demand models and single parameter PSDMs. Per Mangalathu [8], two bridge classes are possible with the selected case study based on the number of columns per bent (1 col bridge and 2 col bridge, hereafter). The initial objective of this study is to check whether ANN approach can predict the demand models without separating the bridge classes. In the second case study, the entire simulation data of all types of the selected bridges are used to compare the efficiency of ANN. Such a study helps to identify whether ANN can possibly avoid the traditional grouping methodology for the generation of fragility curves.

3. Description of bridge structures and assumption of numerical modeling

3.1. Subject bridge class and numerical modeling technique

This research selects two-span, three-span, and four-span concrete box-girder bridges with single-column or two-column bents, and resting on seat abutments. The selected bridges are the typical configuration of concrete bridges in California [8]. A typical layout of their numerical bridge model is shown in Fig. 3, which is created in OpenSees [31]. The decks are modeled with elastic beam-column elements because it would be expected to remain elastic during earthquakes. The effective stiffness for prestressed concrete decks is defined as the gross stiffness (no concrete cracking). The torsional rigidity for a cellular deck is calculated using the rational shear flow theory. The transverse deck elements are modeled using elastic (rigid and massless) beam-column elements to represent the diaphragm of the decks and expansion joints. The deck elements are connected to the columns using rigid elements to ensure the moment and force transfer between adjacent components. Displacement-based beam-column elements with fiber-defined cross-sections are used in this study to model the columns. Fiber cross-sections have the distinct advantage of specification of unique material properties for different locations across a member's cross-section. In the fiber sections (Fig. 3), the *Hysteretic* material model is employed to simulate the longitudinal reinforcement with a hardening factor of 0.01 and the *Concrete02* material model is used to account for the tensile behavior of unconfined (cover) and confined (core) concrete. The confined concrete is simulated using the model of Mander et al. [32]. Foundations are modeled using lumped linear translational and rotational springs (Fig. 3) and are assigned to zero-length elements at the

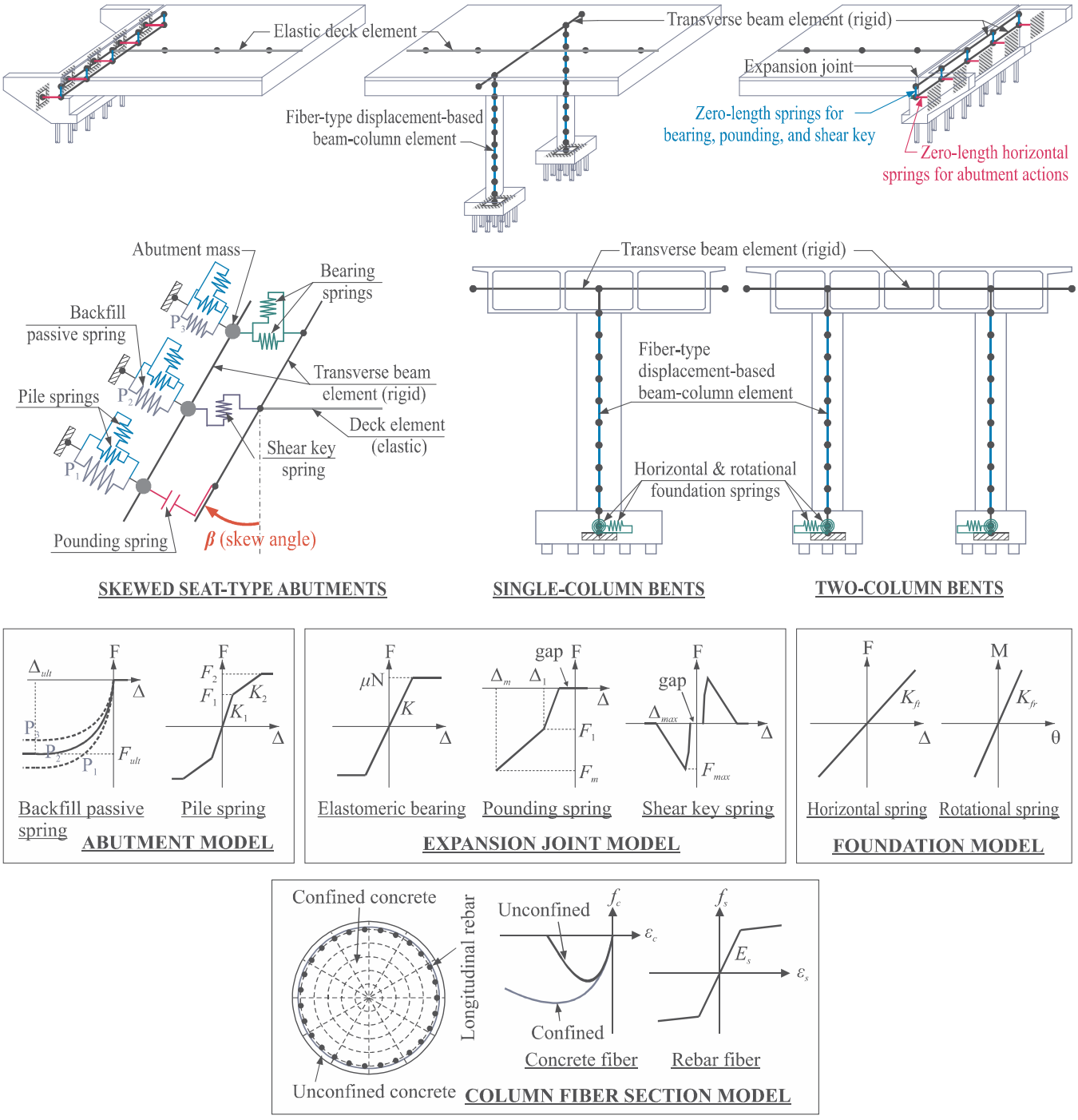

Fig. 3. Computational model of skewed bridges.

center of the footings. These translational and rotational stiffnesses were probabilistically suggested by modeling the foundation systems and various soil profiles in the LPILE program [6] and the values are presented in the following section.

The expansion joint between the deck and an abutment consists of various components such as elastomeric bearings (longitudinal and transverse), shear key (transverse), and pounding between the deck and abutment (perpendicular to the backwall). The elastomeric bearing resists two horizontal forces (longitudinal and transverse bridge axis) and is assumed to be elastic–perfectly plastic and the yield force is computed by multiplying the normal force acting on the bearing with the coefficient of friction of the pad (Fig. 3). The pounding between the deck and abutment restricts the compressive movement because the pounding stiffness is very high, resulting in a little bearing deformation in compression. The pounding is simulated using zero-length elements defined as the material model suggested by Muthukumar and DesRoches [33], which is a nonlinear compression-only bilinear material model with a gap. The direction of the zero-length elements is perpendicular to the backwall plane. This material model explicitly accounts for the loss of hysteretic energy. The initial stiffness and second stiffness obtained from the formulations in the Hertz model are 587 kN/mm and 202 kN/mm, respectively, per deck width (m). The maximum deformation is assumed to be 25 mm and the yield deformation, is assumed to be 10% of the maximum deformation. Two external shear keys per abutment are used to prevent excessive transverse movement of decks. The backbone of the shear key model follows a symmetric

trilinear behavior with a gap, yielded from the experimental results conducted by Silva et al. [34]. The maximum force is computed as the product of the dead-load reaction and the acceleration per the recommendation of the California Department of Transportation (Caltrans) [8]. The yield force is assumed to be 80% of the maximum force and the associated displacement is the gap plus 32 mm. Here, the maximum displacement is the gap plus 160 mm and the corresponding force is zero.

Additionally, the soil and pile springs are rotated with respect to the abutment skew. To account for this abutment skew, the soil model developed by Shamsabadi et al. [35] is modified by changing the maximum force and soil stiffness under the assumption that the direction of the passive pressure is perpendicular to the backwall plane. This model is a compression-only (passive action) hyperbolic material model and the force-displacement curve depends on the backfill type (sand versus clay). Following the work of Kaviani et al. [36], the variation coefficient of stiffness and strength for a specified skew angle (κ_s) is defined as $0.3 \cdot \tan(\beta)/\tan(60^\circ)$. The upper limit of this coefficient is 0.3, which is based on the skew angle of 60°. For example, the modified maximum force at the acute side is the product of the maximum force of the original model and $(1 + \kappa_s)$. It is also assumed that the active and transverse resistance of the abutment is contributed by the piles alone. To capture the nonlinear behavior of the piles, the symmetric trilinear material model is used [8]; the yield force is assumed to be half of the maximum force; and the yield and ultimate deformation are associated with 6 mm and 25 mm, respectively.

As shown in Fig. 3, the components such as the decks, transverse decks, connection between deck and column and between column and footing, and foundation springs are modeled using elastic material models (they are expected to remain elastic during the earthquakes), while other components are modeled in a nonlinear manner. Also, the geometric nonlinearity is accounted for by including P-delta effect on the columns. Rayleigh damping is adopted in dynamic analyses for the first and second vibration modes. Interested readers are directed to the Refs. [8,27] for a more detailed description on the numerical modeling of bridge components.

3.2. Reflecting uncertainties for regional risk assessment

Different sources of uncertainties, such as geometric, material, and system, are included in this research. Table 1 presents the mean value (μ), standard deviation (σ), and the associated probability distribution of various input variables used in this research. The values are determined based on an extensive plan review of bridges (more than 1000) in California [8]. Especially, in the simulation process, skew angles (θ) are uniformly distributed between 0 and 60° (1.047 rad). The input variables are sampled within the range of parameters presented in Table 1 via Latin Hypercube Sampling (LHS) technique to generate samples of bridge models. The sampled values of each uncertain parameter are used as values of input variables in Section 2.2.

To have a wide range of ground motions with a large variation of peak ground accelerations, this research employs the set of 160 ground motions suggested by Baker et al. [37]. The ground motions were proposed for assessing the seismic risk of California. All ground motions in this set are scaled by a factor of two to have sufficient response data of IMs higher than the probabilistic design hazard level in California. Thus, a total of 320 ground motions are used for this research. Following the work of Ramanathan [6], the spectral acceleration at 1.0 s ($S_{a-1.0}$) is adopted as the IM in this research.

Each bridge model is randomly paired with a ground motion with two orthogonal components. One earthquake component is randomly assigned to either the bridge longitudinal or transverse axis. A set of dynamic analyses (320 simulations) is carried out for all bridge-earthquake pairs to monitor the maximum response (termed the engineering demand parameter, EDP) of multiple bridge components. The EDPs considered in this work are the maximum curvature ductility of columns (μ_ϕ), the maximum displacement of the abutments in passive (δ_p in mm), active (δ_a in mm), and transverse (δ_t in mm) direction, the maximum deformation of bearings (δ_b in mm), and the maximum unseating deformation of superstructure (δ_u in mm). These EDPs are regarded as output variables in Section 2.

Table 1
Uncertainty parameters of bridges and their probability distribution [8].

Parameter	Type[a]	Parameters		Truncated limit	
		Mean (μ)	Standard deviation (σ)	Lower	Upper
Superstructure (pre-stressed concrete)					
Main-span length, L_m (m)					
Two-span bridge	N	41.15	10.67	22.86	70.10
Three-span and four-span bridges	N	47.24	13.72	22.86	76.20
Ratio of approach-span to main-span length, ($\eta = L_s/L_m$)	N	0.75	0.2	0.4	1.0
Width of the deck, D_w (m)					
Single-column bent (three-cell deck)	N	12.80	0.61	11.58	14.02
Two-column bent (five-cell deck)	N	17.37	2.44	15.24	20.12
Interior bent					
Concrete compressive strength, f_c (MPa)	N	31.37	3.86	22.75	39.09
Rebar yield strength, f_y (MPa)	N	475.7	37.9	399.9	551.6
Column clear height, H_c (m)	LN	7.13	1.15	5.18	9.75
Column longitudinal reinforcement ratio, ρ_l	U	0.02	0.006	0.01	0.03
Column transverse reinforcement ratio, ρ_t	U	0.009	0.003	0.004	0.013
Deep foundation (pile group)					
Translational stiffness, K_{ft} (kN/mm)					
Single-column bent	LN	350.3	0.44	140.1	875.6
Two-column bent	LN	175.1	0.44	70.05	437.8
Transverse rotational stiffness, K_{fr} (GN-m/rad)					
Single-column bent	LN	9.04	0.28	3.62	22.60
Two-column bent	LN	1.36	0.28	0.54	3.39
Transverse/longitudinal rotational stiffness ratio, K_r					
Single-column bent	LN	1.5	1.5	0.67	1.5
Two-column bent	LN	1.0	1.5	0.67	1.5
Exterior bent (seat-type abutment on piles)					
Abutment skew angle, β (rad)	U	0.52	0.30	0.0	1.05
Abutment backwall height, H_a (m)	LN	3.59	0.65	2.90	6.10
Pile stiffness, K_p (kN/mm)	LN	0.124	0.045	0.058	0.234
Backfill type, *BT* (sand vs. clay)	B	–	–	–	–
Bearing (elastomeric bearing)					
Stiffness per deck width, K_b (N/mm/mm)	LN	0.630	0.299	0.230	1.436
Coefficient of friction of bearing pad, μ_b	N	0.3	0.1	0.1	0.5
Gap					
Longitudinal (pounding), Δ_l (mm)	LN	23.3	12.4	7.6	55.9
Transverse (shear key), Δ_t (mm)	U	19.1	11.0	0	38.1
Other parameters					
Mass factor, m_f	U	1.05	0.06	0.95	1.15
Damping ratio, ξ	N	0.045	0.0125	0.02	0.07
Acceleration for shear key capacity (g), a_{sk}	LN	1	0.2	0.8	1.2
Earthquake direction (fault normal FN vs. parallel FP), *ED*	B	–	–	–	–

[a] N = normal, LN = lognormal, U = uniform, and B = Bernoulli distribution.

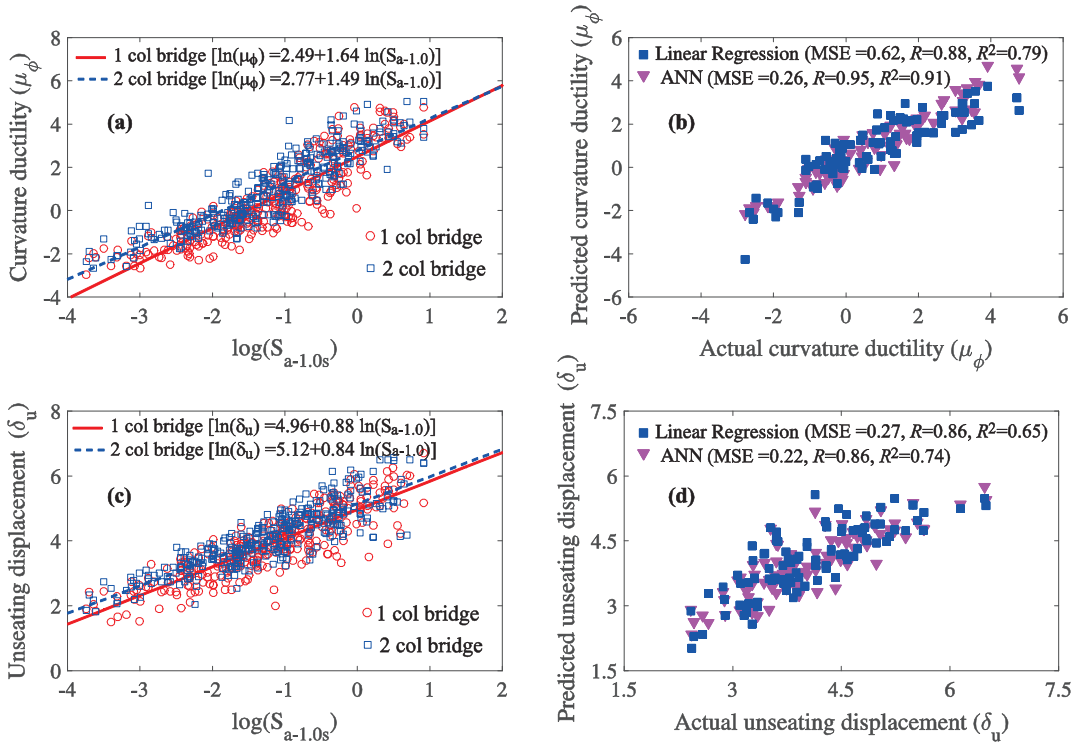

Fig. 4. Results of two-span seat abutment bridges: (a) PSDMs for column curvature ductility, (b) response plots for column curvature ductility for the test set, (c) PSDMs for unseating displacement, and (d) response plots for column unseating displacement for the test set.

4. Application of ANN

4.1. Two-span bridge

Two-span bridges with single-column and two-column bents are initially considered to compare the ANN approach with traditional single parameter PSDMs. As noted by Mangalathu [8], the single-column bent bridges have a statistically different performance in comparison to the two-column bent bridges. It is initially evaluated by comparing the PSDMs and its results are given in Fig. 4(a) and (c). Since the regression coefficients of μ_ϕ and δ_u are different, it can be inferred that they have statistically different performances. The efficiency of the traditional PSDM and ANN is evaluated by comparing their mean square error (MSE), coefficient of correlation (R), and coefficient of determination (R^2) for the randomly assigned test set.

$$\mathrm{MSE}=\frac{1}{n}\sum_{i=1}^{n}(\widehat{D}_{test,i}-D_{test,i})^2$$
$$R=\frac{\mathrm{cov}(\widehat{D}_{test},D_{test})}{\sigma_{\widehat{D}_{test}}\sigma_{D_{test}}}$$
$$R^2=1-\frac{\sum_{i=1}^{N_t}(\widehat{D}_{test,i}-D_{test,i})^2}{\sum_{i=1}^{N_t}(\widehat{D}_{test,i}-\overline{D}_{test,i})^2} \quad (5)$$

where D_{test} is the test set demand vector, $\widehat{D}_{test}$ is the demand vector predicted by ANN or linear regression for the test set, $\mathrm{cov}(\widehat{D}_{test}, D_{test})$ is the covariance of the vector $\widehat{D}_{test}$ and D_{test}, $\sigma_{\widehat{D}_{test}}$ is the standard deviation of the vector $\widehat{D}_{test}$, $\sigma_{D_{test}}$ is the standard deviation of the vector D_{test}, N_t is the training set, and $\overline{D}_{test}$ is the mean value of the demand vector.

It is seen from Fig. 4(b) that for the curvature ductility demand (μ_ϕ), the ANN method can improve the R (from 0.88 to 0.95), R^2 (0.79 to 0.91), and reduce the MSE (from 0.62 to 0.25) compared to the single-parameter PSDM. A similar trend is also observed for the unseating displacement (δ_u) as shown in Fig. 4(d). Although not shown here, in general, ANN can enhance demand estimates significantly for all the demand parameters.

4.2. Two-span, three-span and four-span bridges

As mentioned before, 20 bridge classes with statistically different performances are possible with these bridges. The objective of this study is to check whether ANN approach can have a good prediction model without separating the bridge classes. The results of some selected components (μ_ϕ and δ_u) are presented in Fig. 5. The comparison of ANN and linear regression data for the test set (Fig. 5(b) and (d)) shows that ANN can increase the R^2 and R values significantly and reduce the MSE. As noted before, the bridge groups in the current class have statistically different seismic performance and the traditional linear PSDM cannot capture the variation of structural attributes in the response. For example, for the column curvature ductility demand (μ_ϕ), ANN is able to improve the R^2 and R values by 25% and 13%, respectively. The notable difference between ANN and linear regression is a 73% reduction in MSE. For the unseating displacement (δ_u), ANN increases the R (from 0.84 to 0.96) and R^2 (from 0.75 to 0.93) values, and decreases the MSE (from 0.29 to 0.08). The results are of particular significance as there are lots of structural attributes (that dictate statistically different structural performance) and uncertainties. In other words, ANN is able to have a prediction model even if there are lots of statistically different bridge classes. Such an estimation helps to avoid the grouping of bridge classes before developing demand models and fragility curves intended for a regional risk assessment. In the light of these results, a fragility methodology is suggested and is given in the next section.

5. Fragility functions using ANN and Lasso-Logistic regression

A multi-parameter bridge-specific fragility methodology is suggested in this paper based on the inference noted in Section 4. The proposed methodology has several advantages compared to the existing multi-parameter fragility methods [8,10–17].

(1) The proposed methodology can identify the relative importance of input parameters on the fragility curves. Such identification helps

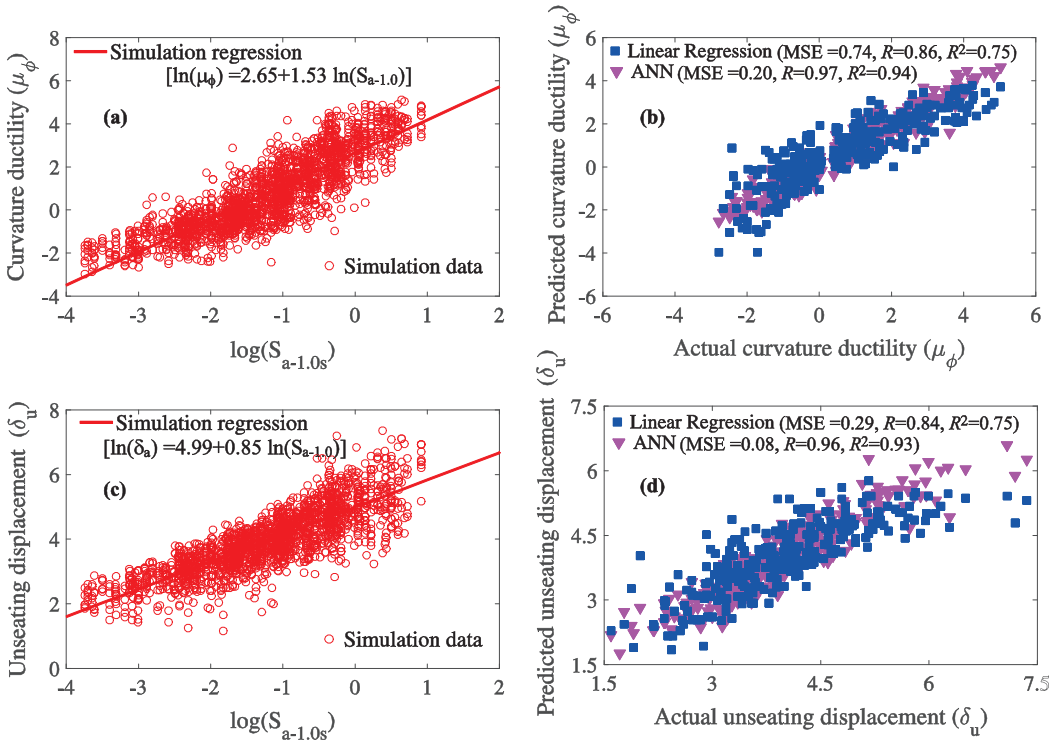

Fig. 5. Results of entire bridge simulations: (a) PSDM for column curvature ductility, (b) response plot for column curvature ductility for the test set, (c) PSDM for unseating displacement, and (d) response plot for column unseating displacement for the test set.

Table 2
Limit state models of various bridge components [8].

Component	Median value, S_c				Dispersion, (β_c)
	Slight (LS_1)	Moderate (LS_2)	Extensive (LS_3)	Complete (LS_4)	
Column curvature ductility (COL)	1	5	8	11	0.35
Passive abutment response (ABP, mm)	76	254	–	–	0.35
Active abutment response (ABA, mm)	38	102	–	–	0.35
Transverse abutment response (ABT, mm)	25	102	–	–	0.35
Bearing displacement (BRD, mm)	25	102	–	–	0.35
Superstructure unseating (UST, mm)	–	–	254	381	0.35

decide whether the uncertainty in the input parameter should be explicitly considered in the generation of fragility curves.

(2) Existing fragility methodology demands the grouping of bridge classes before performing their fragility analysis. The existing grouping methodologies are based either on judgement or computationally expensive statistical procedures. However, the proposed ANN-based methodology does not need any grouping of bridge classes for fragility analysis.

(3) The proposed ANN-based methodology can produce a more reliable demand model even with the large variation in structural attributes and uncertainties in the input parameters. The increase in the R^2 value and the reduction in MSE of ANN are superior in comparison to the existing methods.

(4) Once the trained network for a region located in a bridge is available, bridge-specific or bridge-class fragility curves can be generated with less computational efforts. The fragility curve for a specific bridge can be easily updated using the proposed ANN-based methodology once more information is available from field investigation or database updating.

The outline of the proposed approach is given below:

Step 1: ANN-based demand estimates. (1) Bridge samples accounting for the variation in material, structural, and geometric attributes are created via LHS. Let the input parameters (x_1,…, x_n, *IM*), and the demand parameters be (D_1,…, D_n). (2) The input and demand parameters are assigned into a training set, validation test and test set (3) ANN using the training set and validation set is performed and its efficiency is checked using the test set. If ANN is not efficient, increase the efficiency by increasing hidden layers, the number of neurons, and increase bridge samples. (4) Once the ANN is established, generate a large number of demand estimates (*N*) for each component, k_i, based on their probabilistic distribution. Here, one million samples are used.

Step 2: Capacity estimates. Probabilistic structural capacity models (limit states) for each bridge component are assumed to be log-normal with two parameters (median and dispersion) (see Table 2). Note that the capacity models used here are not a function of structural attributes unlike demand models because experimental tests for most components (except for columns) have been limited. The assumed distributions are used to sample *N* capacity values via LHS.

Step 3: Fragility estimates. (1) The demand estimates from Step 1 are compared with the capacity values from Step 2 to obtain the

binary survival-failure ($N \times 1$) vector. (2) A lasso-logistic regression on the survival-failure vector is conducted to determine the multi-dimensional fragility function of the kth bridge component, conditioned on the input parameters:

$$PF_{k|IM,x_1,x_2,\ldots,x_n} = \frac{e^{\theta_{k,0}+\theta_{k,IM}\ln(IM)+\sum_{j=1}^{n}\theta_{k,j}\ln(xj)}}{1+e^{\theta_{k,0}+\theta_{k,IM}\ln(IM)+\sum_{j=1}^{n}\theta_{k,j}\ln(xj)}} \quad (6)$$

where $\theta_{k,0}$, $\theta_{k,IM}$, and $\theta_{k,j}$ ($j = 1,\ldots, n$) are the logistic regression coefficient of the kth bridge component. (3) As done in the component fragility function, a lasso-logistic regression analysis is repeated to derive multi-dimensional system fragility function by assuming that the bridge failure is a series system (the system fails if one or more components fail). (4) For a particular bridge with input parameters, $x_1,\ldots, x_n$, the traditional one-dimensional fragility curves can be obtained:

$$PF_{k|IM} = \int_{x_1}\int_{x_2}\cdots\int_{x_n}\frac{e^{\theta_{k,0}+\theta_{k,IM}\ln(IM)+\sum_{j=1}^{n}\theta_{k,j}\ln(xj)}}{1+e^{\theta_{k,0}+\theta_{k,IM}\ln(IM)+\sum_{j=1}^{n}\theta_{k,j}\ln(xj)}} f(x_1)f(x_2)\cdots f(x_n)dx_1dx_2\cdots dx_n \quad (7)$$

where $f(x_1),\ldots, f(x_n)$ are the probability density function for parameters, $x_1,\ldots, x_n$.

The limit state models for the various bridge components are given in Table 2, and are consistent with the values reported by Mangalathu [8]. The limit states in Table 2 were determined to facilitate post-earthquake recovery and repair evaluation of bridges. Based on the demand models in the previous section and limit state models mentioned the above, fragility curves using the proposed methodology is developed in the following section. The comparison of the fragility curves generated by the proposed approach with the existing single-parameter fragility curves is also given in the next section.

5.1. Traditional versus proposed fragility curves

Using multi-dimensional demand models and limit state models, fragility curves are generated for a selected bridge class (2-span 1-col bridges). Note that the generation of fragility curves for all the bridge classes is beyond the scope of the current paper and the results are demonstrated with the selected bridge class. However, the proposed methodology can be used to generate fragility curves for any bridge class. To examine the performance of the proposed multi-parameterized fragility model in comparison to the traditional (single-parameter) fragility model, the multi-parameterized fragility function becomes the single-parameterized fragility model by integrating the uncertain parameters as expressed in Eq. (7). Fig. 6 shows the comparison of traditional (single-parameter, unfilled markers) and proposed fragility curves (filled markers) for 2-span 1-col bridges with a skew angle of 20° for selected components (bearing and column curvature ductility).

(1) The proposed methodology provides fragility curves with less dispersion (more reliable) as noted from the shape of the fragility curves. The less dispersion is also quantified in the current study by comparing the standard deviation of the fragility curves after fitting a lognormal distribution. It is attributed to the higher R^2 and lower standard deviation associated with the demand model of the proposed methodology as noted in the comparison of demand models (Figs. 4 and 5).

(2) The reversal of trend (i.e., the failure probability of the traditional method is low at higher IMs) might be attributed to the lower predictive capability of the traditional single-parameter demand model at higher IMs as noted in Figs. 4 and 5. This indicates that the ANN method provides stiffer fragility curves, lower variation in the fragility estimate, and a reliable estimate of the seismic demand and failure probabilities.

(3) The difference in the median values of fragility curves (defined as $S_{a\text{-}1.0}$ at a 50% failure probability) between the two methodologies is 13%, 15%, 9%, and 6% for LS_1 through LS_4. Thus, as the limit state becomes higher, this median difference decreases.

(4) The proposed methodology can be used to generate a bridge-specific fragility curve (for a set of input parameters) without expensive re-simulation. However, the traditional methodology necessities the generation of demand model and fragility curves with the new set of input parameters using a time-consuming dynamic analysis technique.

5.2. Significant parameters affecting bridge fragilities

The proposed approach helps to identify the relative impact of various uncertain parameters on the fragility curves (Step 3 in the proposed methodology). The regression coefficients from logistic-lasso regression are also a measure of the sensitivity of the fragilities to the input parameters. For example, Eq. (6) can be written as

$$\ln\left(\frac{PF_{k|IM,x_1,x_2,\ldots,x_n}}{1-PF_{k|IM,x_1,x_2,\ldots,x_n}}\right) = \theta_{k,0} + \theta_{k,IM}\ln(IM) + \sum_{j=1}^{n}\theta_{k,j}\ln(x_j) \quad (8)$$

The left-hand side of Eq. (8) is called the log-odds and is a linear function of the input variables ($x_1,\ldots,x_n$, IM). The regression coefficients associated with a variable in Eq. (8) can be interpreted as the change in log-odds (or fragility) with a unit increase in the input variable. A positive value of the regression coefficient indicates that a positive increase in the variable increases the failure probability of the component/system (i.e. the system becomes more vulnerable). A negative regression coefficient shows that an increase in that variable reduces the seismic demand. The regression coefficients of 2-span 1-col bridges with different degrees of skew angle for the various damage states are shown in Fig. 7. It is seen from this figure that the ground motion IM ($S_{a\text{-}1.0}$) is the most sensitive parameter, followed by the span length (L_m) and longitudinal reinforcement ratio (ρ_l), for all the demand parameters. For all the damage states, the earthquake direction (ED), damping ratio (ξ), acceleration for shear key capacity (a_{sk}), gap between the deck and shear key (Δ_t), and coefficient of bearing (μ_b) have a minimal impact on all the seismic fragilities. Additionally, the skew

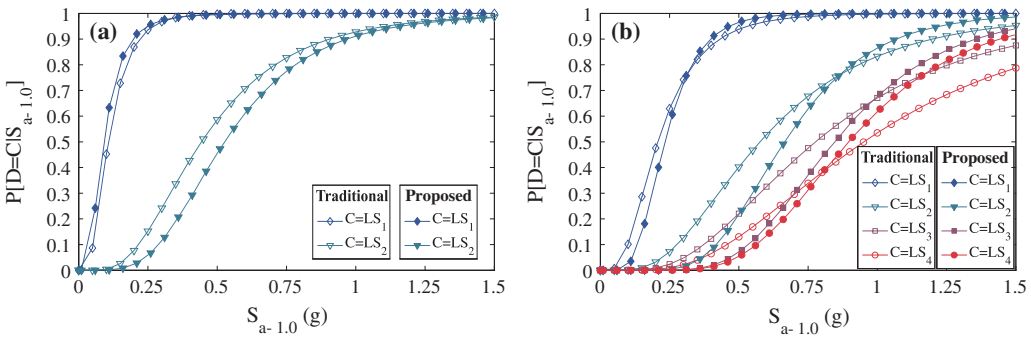

Fig. 6. Comparison of traditional and proposed fragility curves for 2-span 1-col bridge with 60° skew: (a) bearing and (b) column curvature ductility.

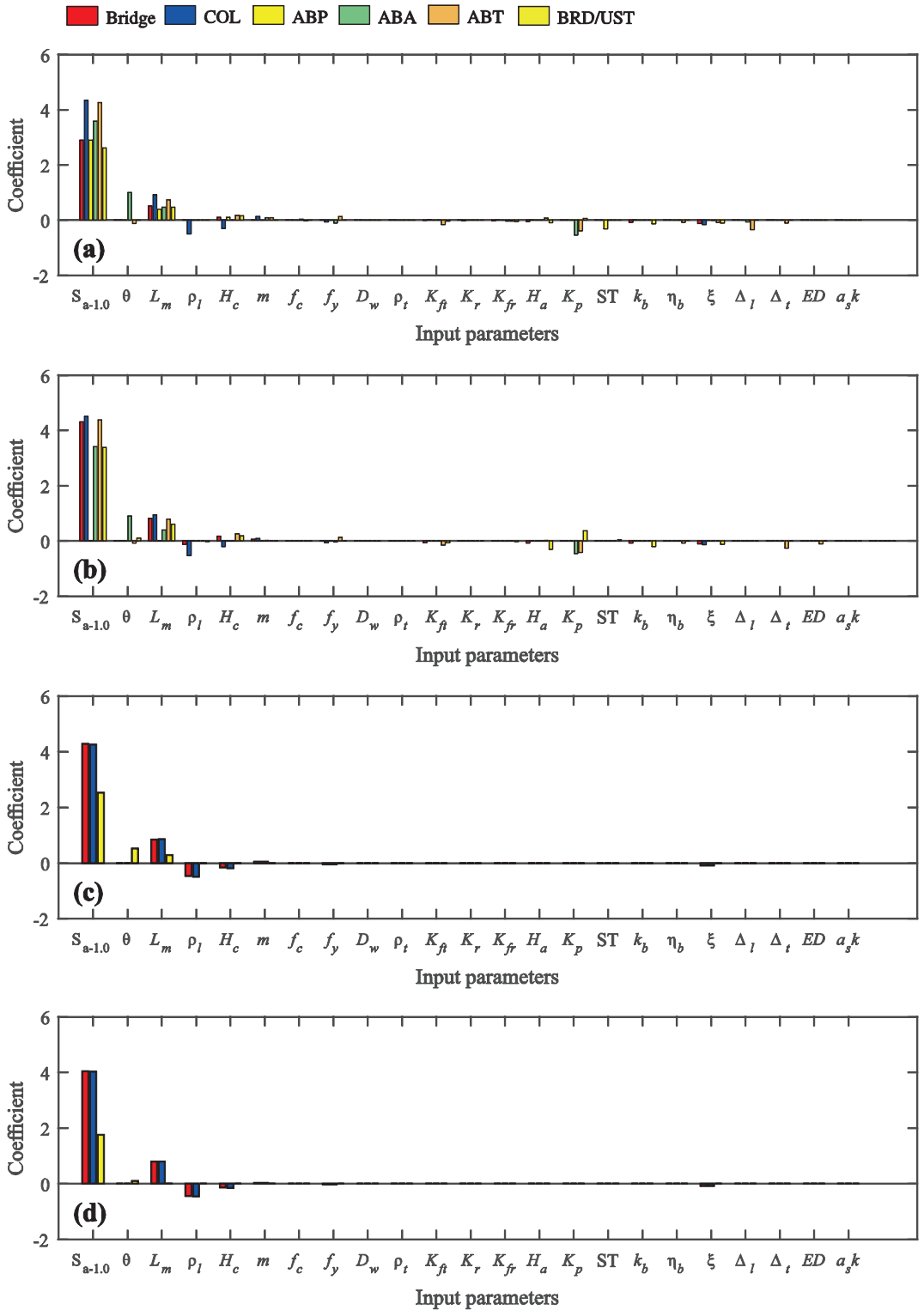

Fig. 7. Relative importance of various uncertain input parameters on bridge fragilities for various damage states: (a) slight, (b) moderate, (c) extensive, and (d) complete.

angle (θ) increases the vulnerability of the active abutment action (ABA), deck unseating (UST), and bearing (BRD) of the bridges. To obtain more insight on the effect of skew, fragility analysis is carried out for 2-span 1-col bridges with four different skew angles and is given in the next section.

5.3. Effect of skew angle on bridge fragility curves

Fig. 8(a) shows the system and component fragility curves for the selected bridge with a skew angle of 20° (2-span 1-col bridges). It is seen that the system fragility is governed by the bearing displacement (BRD) for the selected bridge. Fig. 8(b) shows the variation of system fragility curves with four different skew angles (0°, 20°, 40°, and 60° for the four limit states LS_1, LS_2, LS_3, and LS_4, respectively. Note that the shift of the

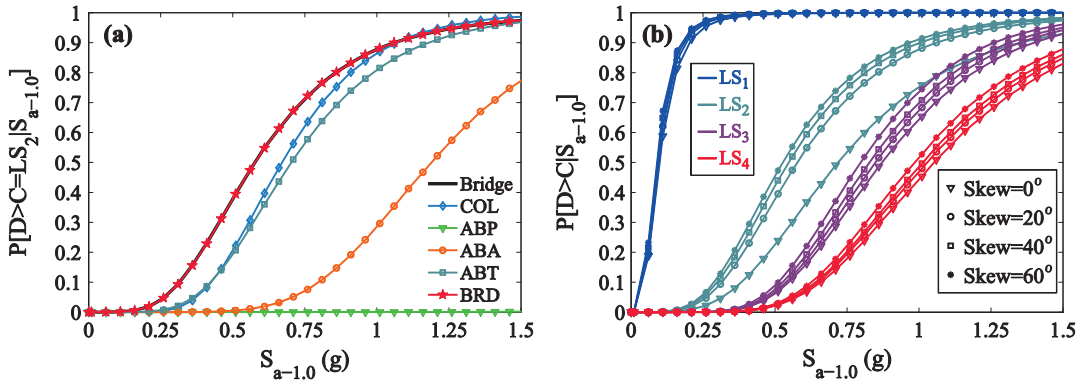

Fig. 8. Fragility curves for 2-span 1-col bridges: (a) system and component curves for moderate damage state (with 20° skew) and (b) comparison of system curves for various damage states (with 0°, 20°, 40°, and 60° skew).

fragility curve to the right indicates the increase of the median value of fragility curves, leading to the decrease of bridge vulnerability. It is seen from Fig. 8(b) that an increase in skew angle makes the system more fragile. The trend is more obvious in higher damage states and it is consistent with the previous work on skewed bridges [27,38]. The system fragility at higher damage states is governed by the columns and deck unseating, which are the main bridge components causing bridge collapse [6–10]. Although skew angle significantly affects the unseating deformation (increase of the unseating deformation), the limit state of the deck unseating is much higher than the seismic demand and thus the contribution of the unseating to system vulnerability is small. Thus, the system fragility is mainly controlled by the column fragility at higher damage states. The generation of fragility curves for the bridge classes with the various configurations considered in the initial part of the paper is beyond the scope of this research, and Fig. 8 shows the demonstration of the proposed approach to generate bridge system as well as component fragility curves. Although the fragility curves are shown here for some selected cases, the proposed methodology can be used to generate fragility curves for a set of input parameters.

6. Conclusions

This paper presents the application of a machine learning technique called artificial neural network (ANN) in the generation of seismic fragility curves intended for regional risk assessment. Existing regional risk assessment frameworks consist of grouping the bridge classes based on their seismic performance and the generation of fragility curves applicable to bridges in a specific class. However, the grouping is based on either engineering judgment or computationally intensive statistical analysis. Also, the grouping of bridge classes varies depending on bridge components under consideration in the process of vulnerability evaluation. The imperative assignment of grouping the bridge classes before performing the regional risk assessment can be eliminated by the ANN-based fragility methodology suggested in this research.

The application of ANN is demonstrated in this research by selecting the two-span, three-span and four-span concrete box-girder bridges with one-column and two-column bents and seat abutments and varying degree of skew angles. It is noted that the ANN-based demand model has higher coefficient of determination (R^2), coefficient of correlation (R) and lower mean square error on the randomly assigned test set. The conclusion holds even if the database used to train the ANN consists of bridge attributes that yield statistically different performance for the bridges. Although 20 different statistically different bridge classes are possible with the selected bridge design attributes (based on the number of span, the number of columns per bent, the degree of skew angles), ANN has a good predictability even if all the attributes are mixed together to estimate demand models.

Based on the insights obtained from the comparison, an ANN-based multi-dimensional fragility methodology is suggested in this research. The methodology also helps to identify the relative importance of each uncertain input parameter on the fragility curves of skewed bridge classes for the first time. For two-span single-column bent bridges with seat abutments, it is noted that the ground motion intensity measure (here, $S_{a-1.0}$), span length, and column longitudinal reinforcement ratio are the most sensitive parameters. It is also noted that the earthquake direction, damping ratio, acceleration for shear key capacity, gap between the deck and shear key, and coefficient of bearing have a minimal impact on all the seismic fragilities. The current study underscores the fact that the traditional single-parameter fragility methodology might not be sufficient to estimate the seismic vulnerability of bridge classes. It is noted that an increase in the skew angle is detrimental to the bridge performance, and the vulnerability increases with the increase in skew angle. This increased vulnerability is more pronounced at the extensive and complete damage states. The proposed multi-parameter fragility methodology helps to generate fragility curves for a specific skew angle and a set of bridge parameters with less computational efforts. Such estimation helps the emergency responders and the bridge inspection team to prioritize their recovery strategies following an earthquake.

Acknowledgements

This research was supported by Basic Research Program in Science and Engineering through the National Research Foundation of Korea funded by the Ministry of Education, South Korea (NRF-2016R1D1A1B03933842). The co-author Gwanghee Heo acknowledges the support by the National Research Foundation of Korea funded by the Korean government (MSIP) (NRF-2016R1A2A1A05005499).

References

[1] HAZUS-MH. Multi-hazard loss estimation methodology: earthquake model. Washington (DC): Department of Homeland Security, FEMA; 2003.
[2] Mangalathu S, Soleimani F, Jeon J-S. Bridge classes for regional risk assessment: improving HAZUS models. Eng Struct 2017;148:755–66.
[3] Mackie K, Stojadinovic B. Probabilistic seismic demand model for California highway bridges. J Bridge Eng 2001;6(6):468–81.
[4] Banerjee S, Shinozuka M. Nonlinear static procedure for seismic vulnerability assessment of bridges. Comput Aided Civ Infrastruct Eng 2007;22(4):293–305.
[5] Banerjee S, Shinozuka M. Mechanistic quantification of RC bridge damage states under earthquake through fragility analysis. Probabilist Eng Mech 2008;23(1):12–22.
[6] Ramanathan KN. Next generation seismic fragility curves for California bridges incorporating the evolution in seismic design philosophy [Ph.D. thesis]. Atlanta (GA): School of Civil and Environmental Engineering, Georgia Institute of Technology; 2012.
[7] Mangalathu S, Jeon J-S, DesRoches R, Padgett JE. ANCOVA-based grouping of bridge classes for seismic fragility assessment. Eng Struct 2016;123:379–94.
[8] Mangalathu S. Performance Based Grouping and Fragility Analysis of Box-Girder Bridges in California. [Ph.D. thesis]. Atlanta (GA): School of Civil and Environmental Engineering, Georgia Institute of Technology; 2017.
[9] Mangalathu S, Jeon J-S, DesRoches R, Padgett JE. Performance-based grouping methods of bridge classes for regional seismic risk assessment: application of

ANOVA, ANCOVA, and non-parametric approaches. Earthquake Eng Struct Dyn 2017;46(4):2587–602.
[10] Mangalathu S, Jeon J-S, DesRoches R. Critical uncertainty parameters influencing seismic performance of bridges using lasso regression. Earthquake Eng Struct Dyn 2018;47(3):784–801.
[11] Seo J, Linzell DG. Use of response surface metamodels to generate system level fragilities for existing curved steel bridges. Eng Struct 2013;52:642–53.
[12] Ghosh J, Padgett JE, Dueñas-Osorio L. Surrogate modeling and failure surface visualization for efficient seismic vulnerability assessment of highway bridges. Probabilist Eng Mech 2013;34:189–99.
[13] Jeon J-S, Mangalathu S, Song J, DesRoches R. Parameterized seismic fragility curves for curved multi-frame concrete box-girder bridges using Bayesian parameter estimation. J Earthquake Eng 2017. http://dx.doi.org/10.1080/13632469.2017.1342291.
[14] Kameshwar S, Padgett JE. Multi-hazard risk assessment of highway bridges subjected to earthquake and hurricane hazards. Eng Struct 2014;78:154–66.
[15] Seo J, Linzell DG. Horizontally curved steel bridge seismic vulnerability assessment. Eng Struct 2012;34:21–32.
[16] Seo J, Rogers LP. Comparison of curved prestressed concrete bridge population response between area and spine modeling approaches toward efficient seismic vulnerability analysis. Eng Struct 2017;150:176–89.
[17] Seo J, Park H. Probabilistic seismic restoration cost estimation for transportation infrastructure portfolios with an emphasis on curved steel I-girder bridges. Struct Saf 2017;65:27–34.
[18] Lagaros ND, Fragiadakis M. Fragility assessment of steel frames using neural networks. Earthquake Spectra 2007;23(4):735–52.
[19] Lautour OR, Omenzetter P. Prediction of seismic-induced structural damage using artificial neural networks. Eng Struct 2009;31(2):600–6.
[20] Mitropoulou CC, Papadrakakis M. Developing fragility curves based on neural network IDA predictions. Eng Struct 2011;33(12):3409–21.
[21] Liu Z, Zhang Z. Artificial Neural Network based method for seismic fragility analysis of steel frames. KSCE J Civ Eng 2017. http://dx.doi.org/10.1007/s12205-017-1329-8.
[22] Pang Y, Dang X, Yuan W. An artificial neural network based method for seismic fragility analysis of highway bridges. Adv Struct Eng 2014;17:413–28.
[23] Haykin S. Neural networks – a comprehensive foundation. India: Pearson Prentice Hall; 2004.
[24] Soleimani F, Vidakovic B, DesRoches R, Padgett JE. Identification of the significant uncertain parameters in the seismic response of irregular bridges. Eng Struct 2017;141:356–72.
[25] Meng JY, Ghasemi H, Lui EM. Analytical and experimental study of a skew bridge model. Eng Struct 2004;26(8):1127–42.
[26] Meng JY, Lui EM. Seismic analysis and assessment of a skew highway bridge. Eng Struct 2000;22(11):1433–52.
[27] Jeon J-S, Choi E, Noh M-H. Fragility characteristics of skewed concrete bridges accounting for ground motion directionality. Struct Eng Mech 2017;63(5):647–57.
[28] Deepu SP, Prajapat K, Ray-Chaudhuri S. Seismic vulnerability of skew bridges under bi-directional ground motions. Eng Struct 2014;71:150–60.
[29] Cornell C, Jalayer F, Hamburger R, Foutch D. Probabilistic basis for 2000 SAC Federal Emergency Management Agency steel moment frame guidelines. J Struct Eng 2002;128(4):526–33.
[30] Wang SC. Interdisciplinary computing in Java programming. New York: Springer Science and Business Media; 2012.
[31] McKenna F. OpenSees: a framework for earthquake engineering simulation. Comput Sci Eng 2011;13(4):58–66.
[32] Mander JB, Priestley MJN, Park R. Theoretical stress–strain model for confined concrete. J Struct Eng 1988;114(8):1804–26.
[33] Muthukumar S, DesRoches R. A Hertz contact model with non-linear damping for pounding simulation. Earthquake Eng Struct Dyn 2016;35(7):811–28.
[34] Silva PF, Megally S, Seible F. Seismic performance of sacrificial exterior shear keys in bridge abutments. Earthquake Spectra 2009;25(3):643–64.
[35] Shamsabadi A, Khalili-Tehrani P, Stewart JP, Taciroglu E. Validated simulation models for lateral response of bridge abutments with typical backfills. J Bridge Eng 2010;15(3):302–11.
[36] Kaviani P, Zareian F, Taciroglu E. Seismic behavior of reinforced concrete bridges with skew-angled seat-type abutments. Eng Struct 2012;45:137–50.
[37] Baker JW, Lin T, Shahi SK, Jayaram N. New ground motion selection procedures and selected motions for the PEER transportation research program. In: Pacific Earthquake Engineering Research Center, University of California, Berkeley, CA, PEER Report 2011/03; 2011.
[38] Zakeri B, Padgett JE, Amiri GG. Fragility analysis of skewed single-frame concrete box-girder bridges. J Perform Constr Fac 2013;28(3):571–82.